Measurement Science and Technology

TOPICAL REVIEW • OPEN ACCESS

Review on sensors for electric fields near power transmission systems

To cite this article: W Hortschitz *et al* 2024 *Meas. Sci. Technol.* **35** 052001

OPEN ACCESS
IOP Publishing
Measurement Science and Technology
Meas. Sci. Technol. 35 (2024) 052001 (17pp)
https://doi.org/10.1088/1361-6501/ad243a

Topical Review

Review on sensors for electric fields near power transmission systems

W Hortschitz[1,*], A Kainz[2], R Beigelbeck[1], G Schmid[3] and F Keplinger[2]

[1] Department for Integrated Sensor Systems, University for Continuing Education Krems, Viktor-Kaplan-Straße 2E, 2700 Wiener Neustadt, Austria
[2] Institute of Sensor and Actuator Systems, TU Wien, Gußhausstr. 27-29, 1040 Wien, Austria
[3] EMC und Optische Strahlung, Seibersdorf Labor GmbH, Campus Seibersdorf, 2444 Seibersdorf, Austria

E-mail: wilfried.hortschitz@donau-uni.ac.at

Received 30 September 2023, revised 16 January 2024
Accepted for publication 30 January 2024
Published 15 February 2024

Abstract

Due to the necessary transition to renewable energy, the transport of electricity over long distances will become increasingly important, since the sites of sustainable electricity generation, such as wind or solar power parks, and the place of consumption can be very far apart. Currently, electricity is mainly transported via overhead AC lines. However, studies have shown that for long distances, transport via DC offers decisive advantages. To make optimal use of the existing route infrastructure, simultaneous AC and DC, or hybrid transmission, should be employed. The resulting electric field strengths must not exceed legally prescribed thresholds to avoid potentially harmful effects on humans and the environment. However, accurate quantification of the resulting electric fields is a major challenge in this context, as they can be easily distorted (e.g. by the measurement equipment itself). Nonetheless knowledge of the undisturbed field strengths from DC up to several multiples of the fundamental frequency of the power-grid (up to 1 kHz) is required to ensure compliance with the thresholds. Both AC and DC electric fields can result in the generation of corona ions in the vicinity of the line. In the case of pure AC fields, the corona ions generated typically recombine in the immediate vicinity of the line and, therefore, have no influence on the field measurement further away. Unfortunately, this assumption does not hold for DC fields and hybrid fields, where corona ions can be transported far away from the line (e.g. by wind), and potentially interact with the measurement equipment yielding incorrect measurement results. This review will provide a comprehensive overview of the current state-of-the-art technologies and methods which have been developed to address the problems of measuring the electric field near hybrid power lines.

Keywords: energy transmission, sensors, electric field, electrostatics, space charge

* Author to whom any correspondence should be addressed.

1. Introduction

Electric fields (E-fields), being relevant in the context of power transmission systems, are either static or in the low-frequency range ($\leqslant 10$ kHz) and can originate from two fundamental sources. Firstly, natural electric fields are caused by the Earth's atmosphere, where a static charge disparity between the ionosphere and the Earth's surface occurs. Under fair weather conditions the static field strength measures around 100 $\mathrm{V\,m^{-1}}$, but immediately before a lightning discharge in a thunderstorm it can rise up to about several 10^5 $\mathrm{V\,m^{-1}}$ [1]. Secondly, there are artificial electric fields, where the most relevant sources are high voltage power systems—particularly, high-voltage power lines. In Europe, for example, the AC field strength at 50 Hz near overhead power lines can reach up to 9 $\mathrm{kV\,m^{-1}}$, while in substations it can exhibit values as high as 18 $\mathrm{kV\,m^{-1}}$ [2].

Due to the shift towards renewable energy sources additional electrical power transmission infrastructure must be installed. The required high-voltage direct current (HVDC) overhead power lines are expected to emit high static electric fields and ionic currents that also cause static or slowly changing (quasi-static) fields. Ground-level DC field strengths can reach values up to about 50 $\mathrm{kV\,m^{-1}}$ [3, 4], accompanied by ion current densities of up to 100 $\mathrm{nA\,m^{-2}}$ [3]. Regulatory authorities had realized the hazardous or disturbing potential of these emissions and they often require companies to measure and specify them [5, 6]. In this context, the relevant dimensions of concern they have identified are:

- **Safety:** The strong electric fields generated by high voltage systems can pose risks to people who come into close proximity with them. By measuring these fields, engineers can determine safe distances from the systems for humans and wildlife.
- **Compliance:** Governmental agencies often require power companies to measure electric fields around power lines to ensure they comply with safety standards and environmental regulations [5].
- **Environment:** Electric fields can affect the behavior of animals and their ability to navigate, communicate, and find food [7, 8]. They do also affect the distribution of particles like dust or liquid droplets in the atmosphere [9–11]. Measuring electric fields can help to identify potential environmental impacts and develop mitigation strategies.
- **Electrical interference:** The electric field of power lines can affect the performance of other nearby electrical equipment, such as communication systems and electronics. By measuring the electric field, engineers can design electrical systems that minimize interference and ensure reliable operation. This is especially critical as renewable energy integration often involves complex electrical networks, where interference can lead to system failures and disruptions [12, 13].

The measurement of the electric field is key in all these aspects. However, low frequency AC fields and especially DC fields are difficult to measure due to a number of issues:

- **Metallic conductors** can effectively shield the electric field to be measured or distort it. Every metallic conductor, being part of the measurement system or the environment, changes the electric field at the measuring site. This affects AC and DC measurements as well.
- All **insulators** used in the measurement device influence the electric field due to their permittivity (AC and DC).
- **Ions within insulators** can migrate under the influence of an electric field. With time constants of minutes or even hours, this process polarizes the material and changes the electric field, causing drift effects in the value measured (mainly DC).
- **Ion currents** in the air can deposit charges on insulating and/or insulated conducting surfaces of the environment or the measurement system and thus generate additional electric fields. These fields superimpose with the field to be measured and, thus, falsify the measurement (mainly DC).

The influence of metals and insulators can be countered by (on-site) calibration. The other issues can be mitigated by appropriate material selection and measurement strategy, but they still are the main reason for serious difficulties and issues.

This paper reviews the current measurement technology for DC and low-frequency AC fields with regard to its possibilities and limitations.

2. Sensing principles for electric fields

The physical quantity the electric field describes is the effect, or force, it exerts on a unit charge. All measuring principles for the electric field are based on this fundamental effect, directly or indirectly. They can be classified into three groups (shown in figure 1) based on the quantity that is exploited:

(i) Mechanical sensors: Force;
(ii) Electrical sensors: Electric current; and
(iii) Electro-optical sensors: Field dependent material parameters.

These principles are discussed in detail below.

2.1. Force-based E-Field sensors

This class of sensors exploits the Coulomb force $\vec{F}$ on a charge Q located on a flexible structure within the electric field $\vec{E}$. As a result, the structure experiences a deflection $\vec{w}$, which for the static case can be simplified to

$$\vec{w} \propto \frac{Q}{k}\vec{E} \propto \frac{\vec{F}}{k}, \tag{1}$$

where k is the spring constant of the flexible structure in direction of the electric field [14, 15].

Despite the intuitive nature of force-based principles it is challenging to develop sensors exploiting this concept. The main reasons are the extremely small forces (in the

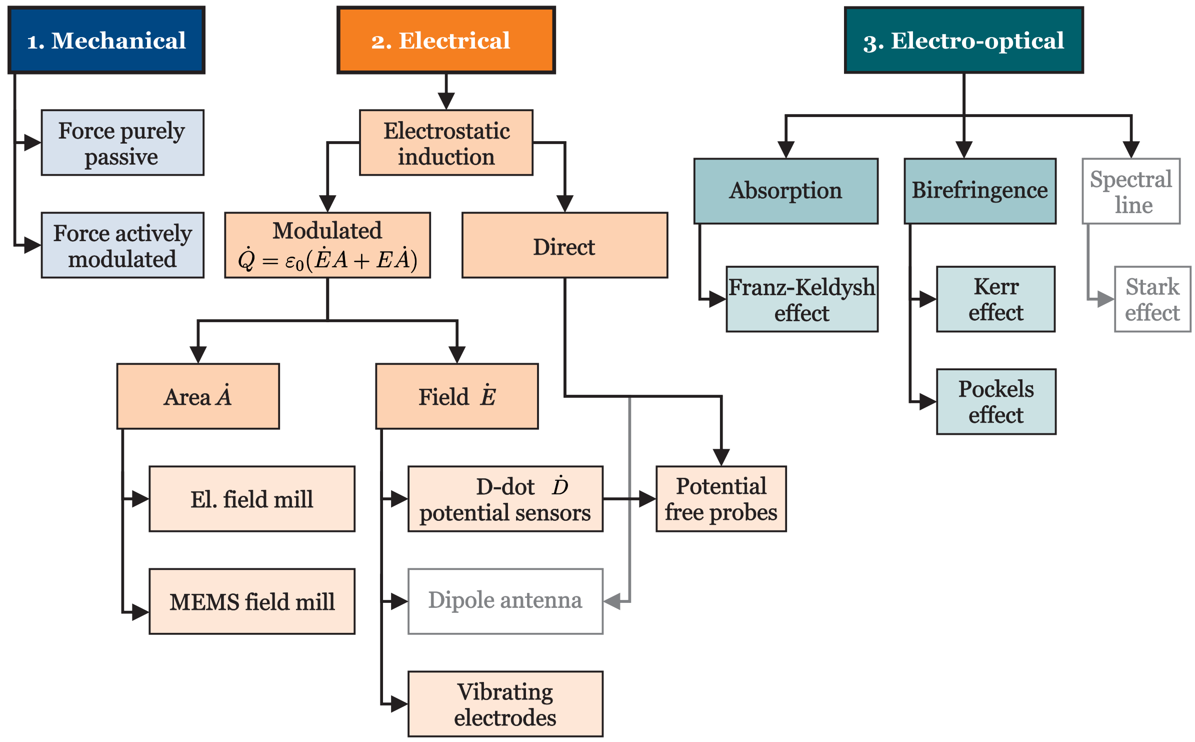

Figure 1. Overview of principles for measuring static and low-frequency electric fields. Items shaded in gray refer to principles that are currently not suitable for DC or low frequency E-fields. Therefore, they are not addressed in this review. Q is the charge involved, A is the area through which the electric field E passes, and D is the electric flux density.

order of piconewtons) and, consequently, the small achievable displacements. Typically, a method capable of resolving picometer displacement is required. Nevertheless, more or less successful attempts to implement this method have been made over the last three decades. These efforts have been driven by advances in technological capabilities and are classified and described for the first time in the following sections.

2.1.1. Principles. Depending on the generation of the charges on the structure, one can distinguish between passive and active force-based systems.

In **passive force-based sensors** (see figure 2(a)), the charges are generated by electric induction of the field to be measured. Since the force is proportional to the electric field strength and the charge, the force on the structure is proportional to the square of the electric field strength ($F \propto E^2$) [16–18]. Therefore, passive systems are non-linear and the polarity of the field cannot be inferred with such a sensor. Additionally, if the field has several frequency components a clear distinction of each original component, weather AC or DC, is no longer possible.

In contrast, **active force-based sensors** (compare figure 2(b)) generate the charges by a voltage source [19–21]. The resulting force in this case is proportional to the voltage and to the electric field with all its components. Thus, it is possible to simultaneously measure harmonics of the electric field and the DC component with its polarity.

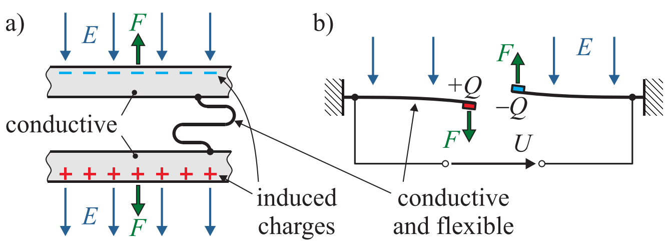

Figure 2. Examples for (a) passive and (b) active force-based E-field sensors. Q is the charge generated by U while E is the electric field and F is the resulting force acting on the flexible structure.

Furthermore, electrostatic induction, as discussed earlier, occurs on all conductive surfaces, including the conductive parts of active systems.

Nevertheless, relatively successful attempts to implement this method have been made over the last three decades. These efforts have been driven by advances in technological capabilities and are classified and described for the first time in the following sections.

2.1.2. Passive force-based principle. An example for this principle was presented by Chen [22] where a grounded, micromachined membrane is supported by four folded springs. This membrane gets deflected in the external electric field as depicted in figure 3. This deflection is transduced by

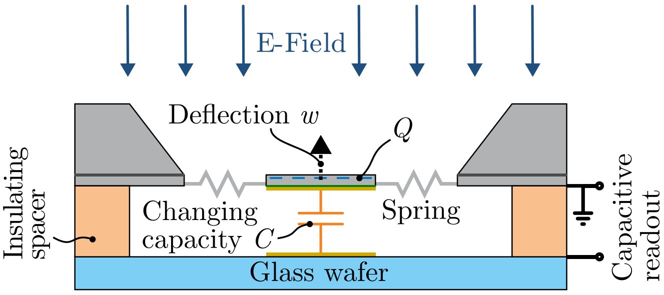

Figure 3. Schematic concept of the passive sensor developed by Chen *et al* (after [22], modified). A deflection is introduce by the electrostatic forces acting on the charges Q induced on the spring supported membrane. The evaluation of the deflection is done with a capacitive readout.

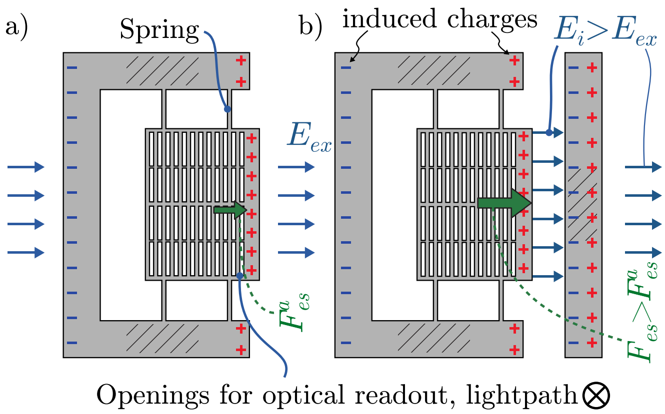

Figure 4. Two concepts of passive micromechanical transducers for electric field sensing. (a) In an external electric field E_{ex}, the force $F^a{}_{es}$ is acting onto the spring suspended, deflectable grating (b) a semi-covered structure enhancing the field (internal electric field $E_i > E_{ex}$ leading to higher forces F_{es} and output signals.

measuring the change of capacitance C between a membrane and an electrode below it. The reported resolution is $16\,\mathrm{kV\,m^{-1}}$. Due to the **capacitive readout**, this sensor type is completely electrical. However, the required voltage for the readout also induces forces on the membrane, which have to be considered.

In contrast to this are **optical readout** methods that do not generate any electrical or mechanical interference. The earliest implementation of such a sensor was published by Priest *et al* [16] where a metal cantilever gets deflected and readout by a **Fabry-Pérot interferometer** (etalon). The entire, cylindrical sensor had a diameter of 2 cm and a height of almost 2 cm. This method was revisited about 20 years later by another group [23]. They miniaturized the sensor by adding a gold ribbon to an optical fiber. The length of the optical cavity between gold ribbon and optical fiber is changed by the electric field. While the measuring range of the sensor described by Priest *et al* in [16] was still limited to relatively high field strengths of $13.5-65\,\mathrm{kV\,m^{-1}}$, with the fiber optic sensor a much more sensitive range of $0.2-3.6\,\mathrm{kV\,m^{-1}}$ was achieved. This was possible by adding metallic 'antennas' that increased the local surface charge on the gold ribbon. The bandwidth was limited to a lower cutoff frequency of about 500 Hz, the measurement of DC fields was, therefore, not possible.

A passive electric field sensor with an **optical aperture** was presented by Kainz *et al* [17, 24–26]. These publications focus on a micro-electro-mechanical system (MEMS) which comprises a moving part made of silicon with an array of holes. On this part, charges are influenced due to the external electric field (figure 4). With a second but static array of holes on a glass chip above the MEMS chip, the light flux between an LED and a photodiode gets modulated by the optical aperture. The measuring range of $70\,\mathrm{V\,m^{-1}}$ to $21\,\mathrm{kV\,m^{-1}}$ was achieved for AC-fields. It was also shown that DC measurements are, in principle, possible when the sensor operates in vacuum to reduce parasitic resistance, albeit at considerable expense and with accuracy $>1\,\mathrm{kV\,m^{-1}}$.

Another passive MEMS structure with a piezoresistive readout was presented by Li *et al* [27] and used in [28] for measurements of AC field strength to back-calculate the voltage on a cable.

Also, **piezoelectric readout** has been applied to quantify the deflections of the movable structure. As these deflections are tiny, so are the voltages that are generated by the stressed piezoelectric material, which is the obvious limiting factor for the sensor's resolution. Huang *et al* [29] have improved the sensitivity for AC measurements by introducing an electret to generate a strong DC bias field. The resulting force on the structure is $\propto (E_{\mathrm{AC}}+E_{\mathrm{DC}})^2 = E_{\mathrm{AC}}^2 + 2E_{\mathrm{AC}}E_{\mathrm{DC}} + E_{\mathrm{DC}}^2$ and, consequently, the force at the frequency of the AC field is linearly proportional to the product of the AC E-field and the DC E-field. A further improvement of this principle enabled a detection limit of $400\ \mathrm{V\,m^{-1}}$ with the prospect of $20\ \mathrm{V\,m^{-1}}$ [30]. However, due to the high DC bias field, this method is basically unsuitable for the measurement of small DC fields.

2.1.3. Active Force-based Principle. This principle requires two electrodes where at least one is on a movable or deflectable structure. The electrodes form a capacitor with the capacitance C, applied voltage U, and charges $\pm Q$ with the magnitude $Q = CU$ generated on the electrodes. In an electric field, the charges and the electrodes both experience the Coulomb force $F \propto QE$. Since the charges are, in general, part of conducting structures, the electric field gets disturbed and the charges do not experience the desired field to be measured. Therefore, the force is $F = \gamma CUE$, where γ is a factor taking mainly into account the aspect ratio of the gap between the electrodes.

Unlike the passive principle, the active one has a linear characteristic, and it offers, additionally, the possibility to control the sensitivity via the voltage U. For example, small field strengths can be made measurable with a correspondingly large voltage and vice versa. Furthermore, this method is inherently suitable to measure static electric fields since the field can be mixed with an AC voltage generating an AC output signal. It has to be noted that this active supply does not necessarily require a grounding of the sensor. The voltage at the

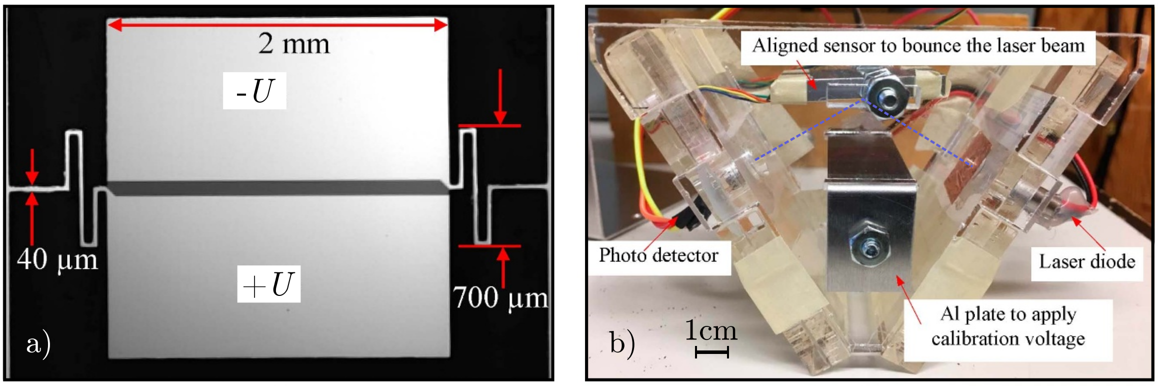

Figure 5. (a) Micrograph of an active force-based MEMS transducer where the structure tilts in an external electric field. $-U$ and $+U$ are the negative and positive voltage with same magnitude applied to the two electrodes on the flexible structure. (b) Acrylic frame holding the sensor membrane and the optical measurement system. The dashed line illustrates the path of the laser light. Modified with permission (CC) from [33].

electrodes can also be generated with a battery. A further discussion about the disturbances caused by grounded elements can be found in section 3.

The active force based principle was first published in 2004 [31, 32], where a micromechanical plate on four springs was used as movable capacitor electrode and a parallel fixed one as second electrode. A newer version from the same group exploits a membrane with two supporting springs that tilts [33]. The two electrodes can be found on a membrane and are supplied by an AC source (compare figure 5(a)). The deflections of the membrane are read out by a very sensitive optical method that can be found in scanning atomic force microscopes. A laser beam is aligned with the membrane at an angle. When the membrane gets deflected, the reflected laser beam changes its position at a differential photodetector (figure 5(b)), affecting the output signal.

Active force-based sensors for electric fields exhibit distinct advantages such as linear response or tuneable sensitivity. Since the forces are very small the readout is challenging and, therefore, these sensors have been developed only within the scientific community, and no commercial devices are currently available.

In the frequency domain, the DC component of the electric field is shifted to the modulation frequency. To avoid ambiguities and asymmetries in the spectrum before and during the reverse transformations, the bandwidth is limited to the difference between the cut-off frequency and the mechanical resonance frequency. Typically, these systems allow for the measurement of low frequency electric fields from DC up to several multiples of 100 Hz.

In general, one can dynamically adjust the measurement range by changing the voltage U at both electrodes (see figure 2(b)).

The minimal measurable electric field is determined by the resolution of the displacement readout and the maximum applicable voltage which in turn is limited by the electric breakthrough field strength between the electrodes. The upper limit of the measurement range is set by the minimum voltage at the electrodes which is larger than the noise floor of the supporting electronics.

With an exemplary, minimal dynamic range of 100 a. u. for the displacement readout and a range for the voltage supply of 1000 a. u., an overall dynamic rage for these type of sensors of 10^5 a. u. is feasible.

2.2. *Sensors based on electrostatic induction*

2.2.1. Introduction. An intuitive method for characterizing electric fields is to use electrostatic induction. It is based on the simplified Gaussian law, which states that the induced charge is equal to the electric flux density multiplied by the area A through which it passes. However, quantifying a static charge (in case of a static field) is challenging for practical reasons. Therefore, the induced current I that flows to or from an electrode due to the influence of the electric field is commonly measured. With the permittivity of vacuum ε_0 the current reads

$$I = \frac{\partial Q}{\partial t} = \dot{Q} = \varepsilon_0 \left(\dot{E}A + E\dot{A}\right) \tag{2}$$

and can be modulated by the temporal changes $\partial E/\partial t = \dot{E}$ and $\partial A/\partial t = \dot{A}$ of the E-field E or the electrode area A, respectively. Both the variation of E and the modulation of A are actively used in various sensing principles, as discussed below.

For example, a rotating shutter changes periodically the influenced charges and generates an AC-current $I = I(f)$ with the frequency f defined by the shutter's rotation speed and the number of wings of the shutter. This corresponds to the second term in equation (2). The most prominent sensor example is the electrostatic field mill (EFM) [34, 35], which exists in many different variants and has been on the market for decades. Nevertheless, specialized systems are still being developed for scientific issues, such as measurement with drones [36] or for the measurement of all three spatial components of the electric field by the usage of additional electrodes [37, 38].

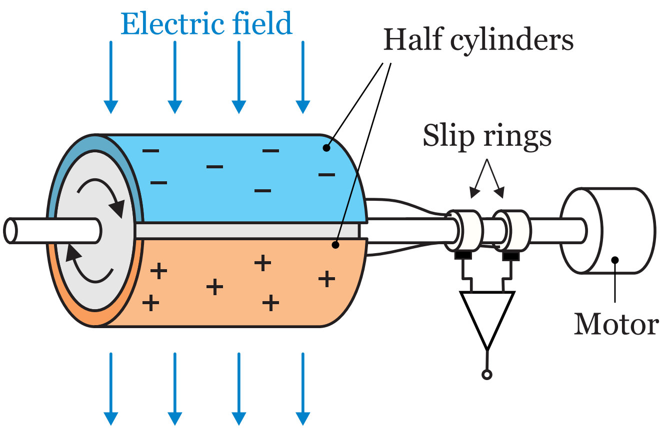

Figure 6. Concept of field mill with rotating electrodes (after [49], modified).

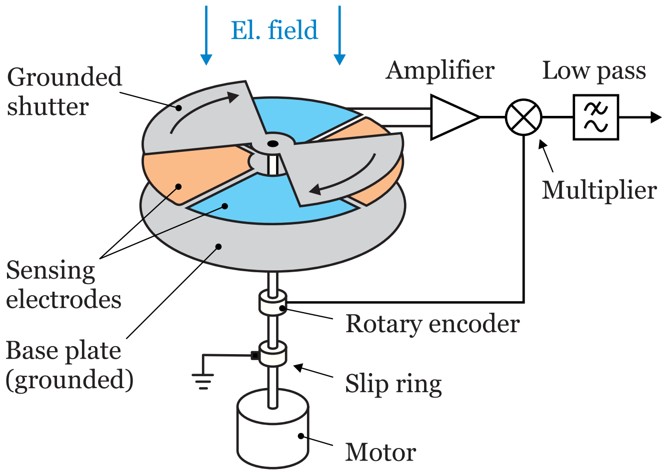

Figure 7. Concept of the field mill with rotating shutter [47].

Sensors that directly evaluate a time-varying field (first term in equation (2)) are, in general, limited to measure AC fields since the induced current is proportional to the frequency of the AC field. The available probes exhibit a lower frequency limit of typically 1 Hz to 5 Hz.

2.2.2. Macroscopic field mills. These sensors are the most common type for measuring low-frequency and static electric fields and have been the standard for monitoring atmospheric electric fields for decades [39–45]. The (quasi-) static electric field strength to be measured, is thereby, converted by mechanical modulation (by a shutter) into an alternating field strength impinging on the measuring electrodes. The alternating induced current at the electrodes is then converted to an output voltage signal by the sensor electronics. This smart approach of generating an alternating quantity from the measured static quantity reduces drift phenomena and enables sensitive measurements (<0.5 V m^{-1} [46]). Using this basic principle, there are three variants described in the literature, which differ in the way of the mechanical modulation [47, 48].

- **Field mill with rotating electrodes:** The typical setup consists of two cylinder halves (electrodes) which are electrically insulated from each other and which rotate in the electric field to be measured (figure 6). While they are exposed alternately to the positive and negative directions of the field, they are generating an alternating signal. Both, vertical and horizontal field components can be measured by determining the phase angle of the AC signal relative to the rotor. In the original version, the electrodes are connected via slip rings adding undesired noise. This drawback was overcome by battery-powered opto-electronics in the rotor [50].
- **Field mill with rotating shutter:** This type involves a stationary measurement in which electrodes are periodically exposed to the electric field by a rotating, grounded impeller (figure 7, shutter) causing AC influenced charges on the electrodes. With, e.g. a lock-in amplifier and the reference signal corresponding to the position of the rotor both, field strength and the polarity of the field, are obtained. This feature is useful on a case-by-case basis when looking for static charges that cause problems in the laboratory or in industrial facilities.
This type of field mill with rotating shutter is very common and commercially available. It is the first choice for measuring atmospheric fields [51] or warning for possible impending lightning strikes (e. g. figure 8 or [52]).
All metallic surfaces of the field mill should be clean, free of contaminants, and not corroded or oxidized, since ions could be deposited on such insulating surfaces and cause interfering fields. Surfaces of or near the sensing elements are, therefore, often plated with gold (compare figure 9) to ensure a well-defined state of the surfaces after cleaning and during operation. This is the method of choice to keep both noise and offset as small as possible. In addition, small gaps between electrodes and shutter should be avoided, as these could produce higher electric fields at the same disturbing voltage level caused by unwanted charges or different contact potentials of metals used [53].

Numerous variants have been developed, differing mainly in the number of measuring electrodes and aperture openings [36, 52, 54–58].

Variants with non-grounded shutter:
The grounded field mill type described in the previous section (compare figure 7) causes a distortion of the field to be measured not only by its conductive parts but also due to the required grounding of the shutter. In most cases, when the environment does not change, this can be counteracted by calibration. But this grounding connection causes wear and additional signal noise. Furthermore, reliable grounding cannot always be guaranteed due to different ground conditions. Field mill types that do not require a defined grounding are therefore of fundamental interest, as this allows mobile application. As early as 1990, J Chubb presented two such types [59]. In both

Figure 8. Example of a compact, commercial EFM system with rotating shutter from Ingesco for fixed outdoor installations as part of a lightning warning system. (In the left picture the rotation of the shutter during image-exposure caused a smearing/blur of its contours.).

Figure 9. Example of a commercial, small, and portable EFM with rotating shutter. The EFM115 from Kleinwächter is read and powered via a USB-connection but needs to be separately grounded during operation.

cases, there are actually two rotors on a common shaft and thus mechanically coupled. Somewhat surprisingly, this publication does not mention the possibility of a mobile application. Furthermore, a commercial implementation was missing for a long time. In 2009, the company of J Chubb (JCI Electrostatic Instrumentation) was incorporated into DEKRA. In the meantime, mobile devices are available, but they still need to be grounded [60].

2.2.3. Scientific field mills. There is a surprisingly small number of recent works, in the scientific literature on field mills, compared to other sensor principles. This could lead to the conclusion that the principle is essentially mature and improvements do not seem worthwhile for the typical applications among researchers.

One of the few recent publications (Cui *et al* [61]) was motivated by the public attention new high-voltage DC transmission lines and their possible environmental impact have attracted. In contrast to high-voltage AC transmission lines, the electric field under HVDC lines is strongly increased when corona discharges occur. Therefore, an accurate and efficient measurement method relaying on field mills has been developed to ensure that the transmission lines meet the electro-magnetic environmental standards. Field mills are manufactured in a large number (65 pieces) especially for this purpose at a technical level close to that of commercial products. The deviations from linearity were reported to be less than 1%, and the accuracy: 2.4%. Since the sensitivity differences between the individual field mills are relatively large ($\approx 2\,\mu\mathrm{V}\,(\mathrm{V\,m^{-1}})^{-1}$, $\approx$10% of the average sensitivity), the listed accuracy is probably only achievable for selected specimens or after careful calibration. The sensitivity of the field mills is strongly influenced by the distance between the grounded rotor and the measuring electrode. If the distance is increased, the shutter also shields larger areas at the edge of the surface of the measuring electrode. Therefore, more and more field lines cannot reach the electrode, but end at the shutter, which decreases the induced charges. For the accuracy stated above the mechanical distances may have a maximum deviation of 50 µm.

The sensor described in the work of Shahroom *et al* [62] was developed for measuring the electric field between clouds and the ground, and is based on the common field mill design. Aluminum and stainless steel were tested as materials for the rotor and electrode, and the results of the calibration process showed that the aluminum type achieved significantly better values for sensitivity, stability, and linearity. Aluminum is coated with a well-insulating oxide layer, a material that should normally be avoided to minimize offset and drift. According to Chubb [59] Gold plating of all surfaces in the vicinity of the sensing electrodes is a simple way to maintain chemical stability. Besides stainless steel, aluminum and gold plated metals also cost-effective PCBs were used in literature [56].

Fort *et al* [46, 63] developed a field mill optimized primarily for low power requirements. For this purpose, a shutter was used, which is actuated by a stepper motor. By measuring only every 40 s, the average power requirement drops to 0.14 W (compared to e.g. 8 Watts from [64]).

The only relevant implementation of the principle with rotating electrodes (as shown in figure 6) was done by Kirkham *et al* [34, 50]. The authors also describe in detail the problem of the finite electrical resistance of the probe holder and the resulting charge transport due to an electrostatic field.

2.2.4. MEMS field mills. One of the main drawbacks of field mills with rotating shutter are the extreme difficulties to miniaturize them since no reliable rotors exist on the micro scale. As a consequence, vibrating shutters have been introduced

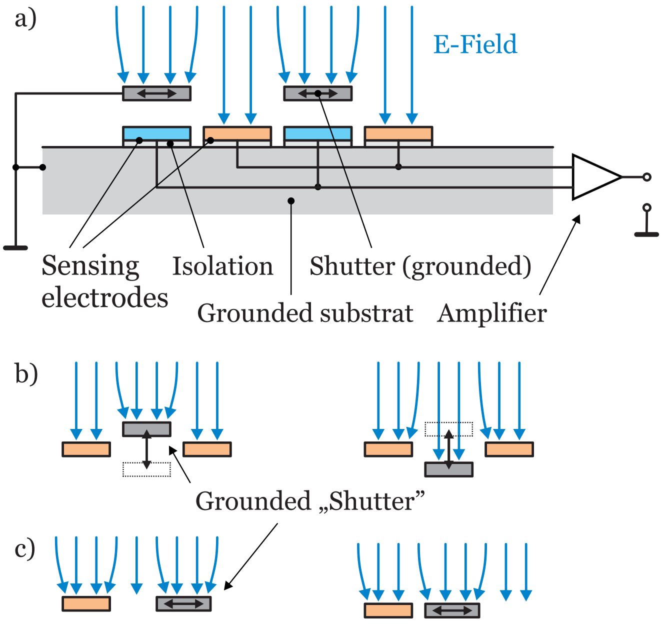

Figure 10. Principles of field mills with vibrating shutter. (a) MEMS version derived from the rotating field mill, (b) structure for out-of-plane vibration, (c) structure for in-plane vibration of the shutter.

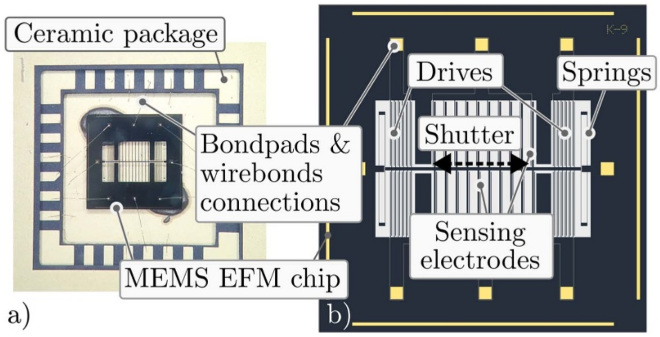

Figure 11. MEMS-EFM (a) fabricated MEMS chip bonded into a package, (b) layout of the chip. The electrostatic drives move the shutter lateral in-plane, shielding the sensing electrodes as also depicted in figure 10(c).

[65–73]. The straight-forward implementation of a vibrating shutter is depicted in figure 10(a), where the shutter shields the respective sensing electrode at a large extend. From the measurement point of view, this is the ideal configuration. However, the technological complexity increases massively because the electrodes have to be fabricated below a moving structure. Figure 10(b) and c depict setups that require only one functional layer, both electrodes and shutter can be fabricated by the same process.

The two setups differ in three relevant aspects. First, the different directions of vibration require different actuation mechanisms. The in-plane structure depicted in figure 10(c) can be excited relatively easily by an electrostatic actuator that is part of the same structure (see also figure 11), whereas the out-of-plane type requires more sophisticated principles (figure 10(b)). Second, the gaps at both sides of the shutter have to be different in the in-plane version; a ratio of 1:10 is common. Therefore, the areal density of sensing electrodes (fingers) is smaller than for the out-of-plane structure by at least a factor of five. And third, the shielding efficiency in the out-of-plane version is higher than in the in-plane version.

As with macroscopic field mills, setups with one measuring electrode (figures 10(b) and (c)) as well as two measuring electrodes (differential mode, figure 10(a) still typically measure only one component of the electric field. Additionally, the shutter can be driven at one of its mechanical resonance frequencies. Large deflections and, thus, large currents due to electrostatic induction are achieved this way. This exploits the mechanical quality factor. The interaction with air is often by far the largest contributor to damping in microsystems. Therefore, MEMS field mills were also tested in vacuum chambers in rarefied air at pressures of e.g. 0.1 Pa to 10 Pa [74–77]. Nevertheless, permanent operation necessitates hermetic encapsulation of the MEMS and, therefore, requires much effort.

A MEMS which is able to measure all three spatial components of the electric field in a single device was introduced by [78]. A piezoelectric actuated MEMS-EFM using a single structure to measure all three components of the electrostatic field was published by [72].

2.3. Displacement current sensors

Another variant of sensors based on the Gauss's Law is capacitive by nature. They are based on the displacement current I_D or the time-varying charge Q induced by the change of the electric field E

$$I_D = \varepsilon_0 A \frac{\partial E}{\partial t} = \frac{\partial Q}{\partial t}\,, \tag{3}$$

where A is the sensor equivalent area [79].

Using the load impedance of the sensor this charge generates a variable potential on a measuring electrode, which can be evaluated by a simple buffer amplifier. Since the displacement current corresponds to the temporal change of the electric flux density $D = \varepsilon_0 E$, this type of sensors is also called 'D-dot sensors'. In the following, various designs of these sensors for low frequencies are discussed in detail, although the applications are often in higher frequency regions such as in lightning detection [80, 81].

2.3.1. Potential-free E-field probes.

The sensor principle (measurement of displacement current, $\dot{D}$) limits such field probes to the measurement of alternating electric fields. Sensitivities of $\approx$1 V m^{-1} and typical bandwidths up to several 100 kHz are obtained with typical sensor sizes of about 100 cm^2. As these devices do not require a ground reference they are portable and allows measurements above the ground plane [82]. The operating principle is currently used by most commercially available electric field measuring instruments

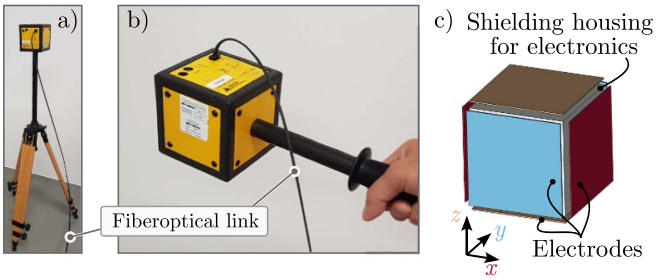

Figure 12. Commercial floating sensor system from Narda (a) on a stand, (b) mounted on a handle. (c) Each pair of electrodes (*x,y,z*) are connected to amplifiers, A/D-conversion and electro-optical-data-transmission inside the housing. The data is transferred to an evaluation device via a fiber optical link.

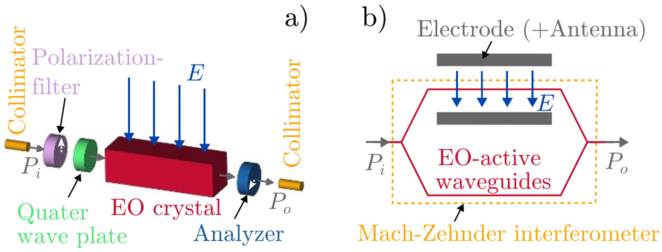

Figure 13. Schematics representing electro-optical sensors. The output power P_o is evaluated relative to the input power P_i. (a) Arrangement for evaluating electro-optical crystals using Pockels effect. (b) Schematic of an fully-integrated Mach–Zehnder interferometer).

for personal protection in the area of AC electric fields. Its realization was already described in the 1970s [83] where these devices were also called 'Free-body meter'. The lower frequency limit for the available probes is between 1 and 5 Hz [84–86] (see also figure 12).

2.3.2. Vibrating reed electrometers. These devices produce an active modulation of the electric field strength by a vibrating measurement electrode behind an aperture in a shielding. The E-field to be measured penetrates through the aperture to the electrode. Since the field strength inside the shield decreases with increasing distance from the aperture, an AC current is induced by vibrating the electrode and changing the distance from the aperture to this electrode.

Commercial implementations of this measurement principle can be found in [87–89]. These devices are used, e.g. in process monitoring and surface testing. A prominent example from academia is the work of Kobayashi [90–92], who uses two piezoelectric elements, one to drive the sensing electrode and one to read its position. This is required for 'self-excited vibration' and for demodulating the signal from the influenced charges on the sensing electrode after amplification.

2.4. Electro-optical sensors

2.4.1. Introduction. When a dielectric is placed in an electric field, it becomes polarized and for special materials, this leads to a change in their material properties. By quantifying these changes this provides a means to measure the electric field. Optical properties are especially promising candidates for this concept. The most important class of materials here are electro-optically (EO) active crystals, which alter either absorption or refraction properties [93–96]. Since these materials are dielectrics, the distortion of the field to be measured is minimal. But, in principle, no conductive and grounded connections are required for the measurement probe. Due to the very fast response time of these materials, high bandwidths up to THz are achievable [97]. The following effects are exploited:

- The change in **optical absorption** due to E-fields is called the **Franz-Keldysh effect**. It has significance only in the communication technology, where optical signals are switched by applying fields in the range of 100 kV m^{-1} to 1 MV m^{-1} [98, 99]. For the measurement of E-fields, it plays only a minor role.
- The influence of the electric field on the **refractive index** n can be described by a series expansion

$$n(E) = n_0 + S_1E + S_2E^2 + \ldots, \tag{4}$$

where n_0 is the refractive index without field [93, 100]. Omitting terms of higher order than the first, the change of n can be expressed by $\Delta n = S_1E = -1/2n_0^3 r_{\text{eff}}E$, where r_{eff} is the so-called electro-optic coefficient. This first order effect is called **Pockels effect** (see also figure 13(a)). The factor S_2 describes the quadratic dependence and is referred to as **Kerr effect** [101–103]. It can also be written as $\Delta n = S_2E^2 = \lambda KE^2$, where λ is the wavelength of the light and K is the Kerr constant. The Kerr effect is orders of magnitude smaller than the Pockels effect [94, 100] and is applied almost exclusively at large E-fields. Also liquids such as transformer oil act as the electro-optic medium [104]. Which of the two effects occurs depends on the symmetry and structure of the electrical polarization (polarization density) [105]. The effects are discussed in 2.4.3. Higher order terms than S_2 are generally not exploited since they are again orders of magnitude smaller [94].

Electro-optic materials enable measurements of electric AC-fields, but these materials are not suitable for DC fields. As an example the commercial system from Kapteos has a frequency range from 40 Hz up to 30 MHz [106]. Such systems are almost exclusively used in the scientific field for highly accurate measurements of AC fields with minimal distortion of the field [107]. The literature focusing on the measurement of DC fields states that very accurate temperature control ($<$0.2 K) is necessary to achieve stable measurements [105, 108, 109]. Additionally, without knowledge of the strength of the DC field, direct measurement of combined DC and AC fields is not possible, as the DC field affects the sensitivity of the AC measurement [110].

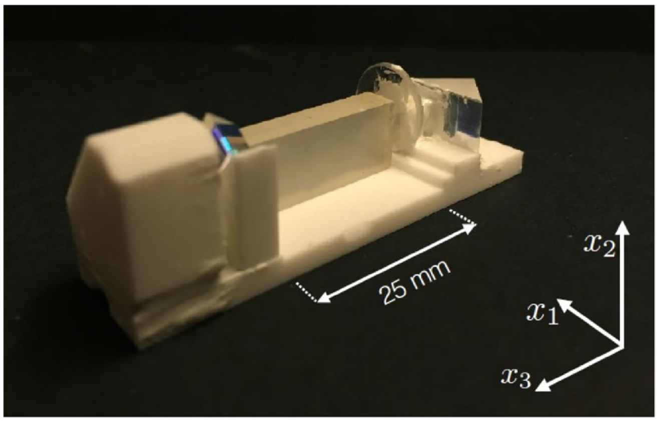

Figure 14. Photograph of the electro-optic electric field sensor used by Grasdijk *et al* [108]. The optical fibers connecting to a light source and to two photo-diodes are not shown. Laser light is transported via an optical fiber (from the left, not shown) is collimated in a lens, and reflected and displaced by a prism to run in parallel to the incoming beam. It passes a linear polarizer, a $\lambda/4$ plate and a 25 mm long $LiNbO_3$ crystal. With permission (CC) from [108].

Furthermore, Cecelja *et al* [111–113] showed that the sensitivity of the electro-optical measurement system changes significantly under the influence of space charges. Therefore, without knowledge of the nature and density of these charges, it is not possible to measure the original field. Due to these problems, electro-optical sensors are, currently, not suitable for electric fields in the vicinity of hybrid power lines.

2.4.2. Evaluation principles. The change in refractive index caused by an electric field can affect various properties of a light beam passing through a crystal, including its amplitude, phase, polarization state, or frequency, as documented in [94]. When phase information is crucial, the use of coherent light is mandatory. Typical measurement principles are:

- Evaluation of **optical phase shift** with Mach–Zehnder interferometers [114–121] (compare figure 13(b), which are also used in commercial systems as offered, e.g. by SRICO [122].
- Determination of **refractive index changes** of electro-optic crystals using a cavity [123]. The optical path length of the crystal within the cavity is changed by the electric field, leading to a strong interference effect as the light passes the crystal multiple times [124].
- Measuring the altered **polarization state** of circularly polarized light that is directed through the electro-optic crystal. The applied electric field changes the phase delay between two orthogonal components of the light beam [125]. In practical applications, polarization filters transform the phase delay into changes in optical power [126–128] (see figures 13(a) and 14).

Regardless of which of the three principles is applied for measurements, finally intensity changes are determined by one or more optical receivers [94].

2.4.3. Materials. For the electro-optic measurement of electric fields only a limited number of materials exist. The most important ones are electro-optic crystals, they are listed below. According to Brinkman [100] the EO-coefficients strongly depend on the orientation and wavelength of the light and the orientation of the electric field. Furthermore, the values depend on the mechanical fixation (clamped and free) which is often not discussed in the literature. Since the aim is not to provide a complete tabulation of all material parameters, only orders of magnitude are given here to show the advantages and drawbacks of the various materials:

- **Lithium niobate** (LN, $LiNbO_3$) is the most commonly used material in electro-optic sensing and has an anisotropic crystal structure with 3 m point symmetry. Temperature stability, as explained in [113], is primarily influenced by the temperature-dependent natural birefringence, which can be further affected by the pyroelectric effect. The impact of both effects can be minimized by precise crystal alignment with the optical axis. Any misalignment during measurement can deteriorate the temperature stability. To mitigate the effects of birefringence, Cecelja *et al* recommend aligning LN crystals within 0.01° to the optical axis [113]. Compared to other EO-materials, LN exhibits a relatively high permittivity of 85 and low electrical conductivity. The index of refraction for LN is 2.2 [129, 130]. The EO coefficient r33 is in the order of 31 pm V^{-1}. LN features a very high charge relaxation time constant of 7×10^6 s [93]. The costs for crystals made of LN are approximately half of the one of Lithium tantalate and a fraction of the one of Bismuth germanate.
- **Bismuth germanate** (BGO, $Bi_4Ge_3O_{12}$, $Bi_{12}GeO_{20}$), as cited in [104, 109, 125, 131], is also often used in electro-optic sensing. It has a rather low relative permittivity of 40 [129] and a cubic crystal structure with $\bar{4}3$ m point symmetry, resulting in no induced natural birefringence. Consequently, BGO inherently exhibits high temperature stability [113]. BGO exhibits an OE coefficient r41 of 3.8 pm/V [129]. According to Bordovsky it has a low charge relaxation time of 248 s.
- A less commonly used material is **Lithium tantalate** (LT, $LiTaO_3$) [93] that allows for simultaneous measurement of two field components [132]. The index of refraction for LT is 2.18 [129, 130]. The EO coefficient r33 is in the order of 30 pm V^{-1} while the associated permittivity is 45.
- **Bismuth silicon oxide** (BSO), related to BGO, has been utilized for DC measurements [133] and enables also the simultaneous measurement of two field components perpendicular to the light path [134]. BSO has an EO coefficient r41 of 4.1 pm V^{-1} and a permittivity of 56 while the refraction index is 2.5 [129]. It features very low charge relaxation time constant of 0.28 s [93].

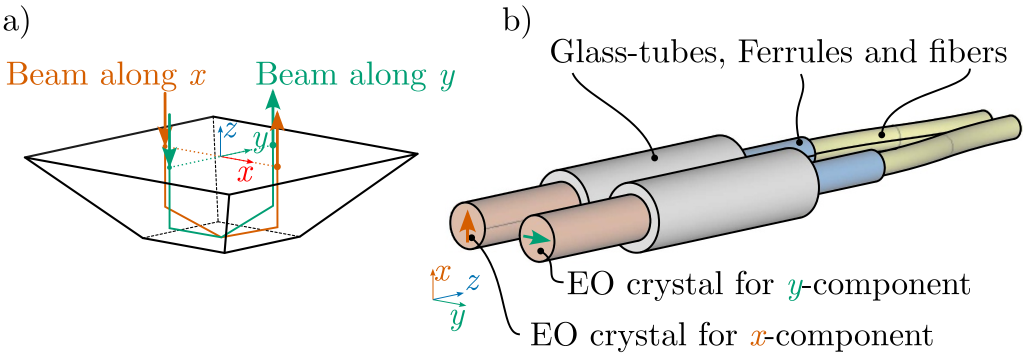

Figure 15. (a) The 'Total-Internal-Reflection'-sensor made of LiTaO3 with four angled surfaces after [132] uses two separate laser beam paths to measure the two E-field components in the $x-y$-plane. (b) Schematic of a pigtail EO transducer with two crystals with different orientations according to [145].

- Compared to the listed inorganic materials organic ones like **EO polymers** exhibit a beneficial low permittivity [135]. Zhang *et al* [120] tested a polymer specifically for AC applications with strong fields. EO polymers can exhibit very high EO coefficients of up to 300 pm V^{-1} [136–138] while the refraction index is in the order of magnitude of 2. Another example is discussed in [139], where an integrated waveguide Mach–Zehnder interferometer exploits an EO-polymer placed on a coupled micro-ring resonator. Despite recurrent publications, EO polymers are not commonly employed in practical applications and literature lacks information on their material lifespan and costs, in contrast to crystals.

The Pockels effect is primarily utilized in inorganic crystals, with occasional use in organic compounds like polymers [104]. The Kerr effect is in EO measurement technology mainly exploited in liquids [105] and used as a nonintrusive method to study, e.g. breakdown mechanisms in transformer oils [140, 141] or to examine insulating liquids [142, 143] in large electric fields of more than 10 MV m^{-1}. Duvillaret, along with Cecelja and Hidaka [105, 113, 144], extensively discuss the variations among the most common crystals employed for electric field measurements. These discussions cover the crystal type, refractive index, relative permittivity, and the optimal orientation to minimize unwanted side effects. It is important to note that material defects and impurities in these crystals can increase their conductivity, making them less suitable for stable DC measurements. When using materials without natural birefringence, the temperature dependency of the electro-optic material, as highlighted by Kumada and Hidaka [109], becomes negligible.

2.4.4. Measurement systems for AC fields. There are different approaches for measuring two field components: First, applying multiple and orthogonally arranged EO sensors, second, choosing crystals exhibiting independent change of the refractive indices in different spatial directions (e. g., BGO and BSO) [133, 145, 146] (compare figure 15(b)), and third, using two laser beams that are guided through a specially formed crystal along different paths [132] as depicted in figure 15(a). Due to the fixed direction of the incident light in fiber optical systems, only two components of the electric field vector can be measured.

Simultaneously measuring all three components of the electric field with fiber based systems requires at least a combination of two crystals, as shown in [145]. Alternatively, three individual sensors with only one sensitive axis can be combined into a composite probe [147]. As mentioned earlier, it is possible to significantly reduced the temperature sensitivity of EO materials by carefully selecting the crystal orientation [113]. However, the temperature stability of essential components like polarizers cannot be compensated by the orientation of the crystal. In such cases, automatic compensation techniques with servo-controlled optical components are applied [126, 148]. Although this approach increases complexity, it is used in commercial products, such as those from Kapteos.

2.4.5. Measurement systems for DC-fields. Measurements of DC fields have been performed for decades [93, 111, 149], but mostly no clear estimation of long-term stability was done. Commercial devices that can measure DC fields in a dedicated way do not exist until today [108]. One reason for the difficulties in measuring DC fields are the dielectric relaxation effects in the electro-optical crystal found by Garzarella *et al* [150]. Grasdijk *et al* [108] demonstrated that the relaxation process can extend from a scale of seconds to hours by minimizing the crystal's temperature dependence using LN (Y-Cut). However, the authors also emphasized that temperature stabilization ($\Delta T < 0.2$ K) is essential for long-term DC measurements. Combined with averaging over 5 s, a resolution of 400 V m^{-1} was achieved. Yang *et al* [151] used a rotating conductive shutter over the EO sensor to measure hybrid fields, but the DC measurement capability was achieved by sacrificing the main advantage of EO sensors, the minimal field distortion due to the lack of grounded metallic components (compare figure 16).

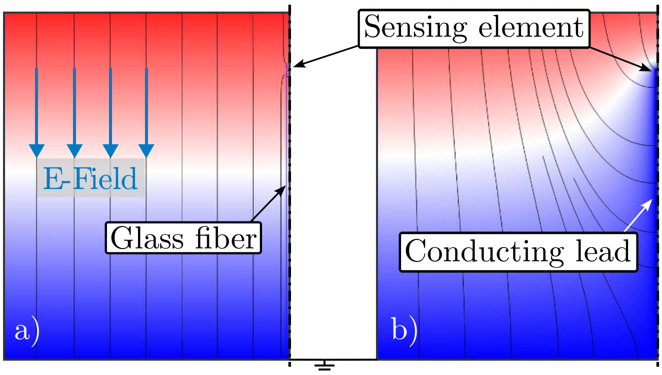

Figure 16. Distribution of the electric potential: (a) almost undisturbed around a dielectric sensor and (b) massive distortion by a conductive connection from the sensor to ground potential.

3. Calibration

A fundamental problem of electric field sensors is the field distortion they cause (see figure 16). This effect is hardly avoidable but can be counteracted by calibration. Sensors are usually calibrated at the factory using the parallel plate setup. The applied voltage generates a homogeneous electric field between the plates [152–155]. The sensors are then typically placed between the plates. In the particular case of calibrating field mills, a hole in the center of the grounded plate is made and the opening of the field mill is mounted flush with this plate. To minimize edge effects, plates with a diameter of about 1 m are typically used with a spacing of about 16 cm. The plates are made of polished stainless steel to reduce the unwanted occurrence of surface charges on dielectric oxides and to ensure a stable zero electric field. Sharp corners must be avoided to prevent corona discharges at higher field strengths. Surrounding surfaces should be grounded, while the insulated inner plate is fed by a high-voltage amplifier. This amplifier must be calibrated annually off-site, to achieve the required accuracy (e.g. using technology traceable to the National Institute of Standards and Technology).

3.1. Calibration under the influence of space charge

The calibration of field mills, specifically in the presence of space charges near DC/AC electric power transmission lines, is addressed in [54, 156–158]. Nevertheless, until now, no commercial device is known to the authors which is capable of working reliably under the influence of space charges. The works of [111–113] addresses in detail the measurement of DC fields with EO affected by corona discharges. The sensitivity of the measurement system varies due to unipolar and bipolar charge carriers, but remains proportional to the space charge density. The linearity of the system is maintained at constant discharge ratios. The normalized output changes from about 4.5 per kV/mm for pure DC fields to about 0.6 per kV/mm for DC fields with positive charge carriers and further to about 0.17 per kV/mm-1 for DC fields with bipolar charge carriers. According to [111], understanding the kind and density of charge carriers is critical for measurements that are affected by them. To reduce the effects of surface charge carriers, researchers suggested rotating the optical crystal in the field during DC measurements [149, 159–162]. However, this symmetrical charging of the transducer remains effective only when the ion current is uniformly distributed which is not the case under an outdoor power transmission line.

4. Summary

The necessary shift to renewable energy to reduce the emission of greenhouse gases requires the construction of new power transmission lines. These lines are essential to distribute energy from emerging, distant energy sources such as offshore wind farms. Some of these new DC transmission lines will run alongside the existing AC lines to further use already existing corridors, avoiding lengthy approval procedures for new ones. To meet safety, compliance and environmental standards, it is essential to measure the electric fields in the vicinity of these new hybrid transmission lines. Since hybrid transmission lines emit charge carriers, special sensors capable of operating in the presence of charges are needed. In this article, all methods and systems under consideration have been examined for their suitability for measuring AC and DC fields including their reliability in the presence of ions or space charges. In summary, a variety of measurement methods exist for measuring either low-frequency or DC electric fields. Several of these methods are also available as commercial products and generally cover specific application areas.

For quantifying DC fields, electric field mills are the established instruments. In contrast, microsystem-based EFMs, and force-based microsensors, are primarily in the prototype phase of scientific investigation. This is due to the need for additional protective layers to safeguard the fragile, mechanical structures from environmental factors like dust, moisture, rain, or insects. However, the stable operation of EFMs (in environments with space charge) requires grounding, which in turn affects the field being measured (and the charge distribution).

Although potential-free probes are highly advanced devices, their principle of operation restricts their use to the characterization of AC fields. For measurements in the vicinity of high-voltage lines, they excel through mobile usage without grounding.

For the outlined application under hybrid power transmission lines, electro-optical systems currently can be employed exclusively for characterizing AC fields. The advantages of EO systems include their compact size and the dielectric material of the probe while no grounded elements are necessary (for AC measurements). Additionally, with appropriate choice of the material a single sensor can provide 2D measurements. However, DC measurements still require extensive efforts such as intense temperature stabilization and are, therefore, currently only investigated in the scientific field. This includes methods to mitigate the impact of space charge on EO systems.

Extra equipment, typically Wilson plates, are used to assess the ion currents produced around hybrid transmission lines. However, due to their fixed installation on ground level, their size and the required earthed guard rings, simple mobile handling is not feasible.

Finally, up to now there is no compact, 'all-in-one' measurement system for hybrid DC and low-frequency electric fields (within the required frequency range up to 1 kHz) available. Furthermore, all available systems for measurements of the DC field are not immune to the accumulation of space charges during the measurements and usually need to be grounded during operation. This inherently leads to distortions of the electric field or even an increase in the field around the instrument, which in turn causes air ions to be transported to the instrument. Therefore, present measurement equipment for the vicinity of power transmission lines is still installed below ground level to avoid these influences. Quantities like the ion-current-density are separately measured with Wilson-plates. These circumstances pose challenges for the work in the field of 'daily immission measurement'. Further research and development are still necessary to simplify required equipment needed for measuring the electric field without the influence of space charges. These devices should function without disturbing the field to be measured or at least without having them to be installed below ground beneath hybrid high-voltage lines as it is done today [3, 163–165].

Data availability statement

All data that support the findings of this study are included within the article (and any supplementary files).

Acknowledgment

This work is co-funded by the Gesellschaft für Forschungsförderung Niederösterreich (GFF/NFB) within the project FTI19-019, the county of Lower Austria, the EU and the Project FKZ3619S92411 for the Bundesamt für Strahlenschutz.

ORCID iDs

W Hortschitz https://orcid.org/0000-0003-2950-642X
G Schmid https://orcid.org/0000-0002-3435-6844

References

[1] Kolmašová I *et al* 2022 Continental thunderstorm ground enhancement observed at an exceptionally low altitude *Atmos. Chem. Phys.* **22** 7959–73

[2] Hirtl R, Schmid G and Friedl K 2018 Expositionsbewertung in hochspannungsanlagen - numerische berechnungen der im körper induzierten elektrischen feldstärke für unterschiedliche praxisrelevante expositionsszenarien *NIR 2018: Wellen-Strahlung-Felder* pp 585–99

[3] Sarma Maruvada P 2012 Electric field and ion current environment of HVdc transmission lines: comparison of calculations and measurements *IEEE Trans. Power Deliv.* **27** 401–10

[4] Liu J, Zou J, Tian J and Yuan J 2009 Analysis of electric field, ion flow density and corona loss of same-tower double-circuit HVDC lines using improved FEM *IEEE Trans. Power Deliv.* **24** 482–3

[5] European Commission 2013 Directive 2013/35/eu on minimum health and safety requirements re-garding the exposure of workers to the risks arising from physical agents (electromagnetic fields) *Official J. Eur. Union*

[6] Council of the European Union 1999 *Council Recommendation of 12 July 1999 on the Limitation of Exposure of the General Public to Electromagnetic Fields (0 Hz to 300 GHz)* (Publications Office of the EU)

[7] Clarke D, Morley E and Robert D 2017 The bee, the flower and the electric field: electric ecology and aerial electroreception *J. Comp. Physiol.* A **203** 737–48

[8] Hunting E R *et al* 2021 Challenges in coupling atmospheric electricity with biological systems *Int. J. Biometeorol.* **65** 45–58

[9] Toth J R I I I, Rajupet S, Squire H, Volbers B, Zhou J, Xie L, Sankaran R M and Lacks D J 2020 Electrostatic forces alter particle size distributions in atmospheric dust *Atmos. Chem. Phys.* **20** 3181–90

[10] Wen X, Yang P, Chu Z, Peng C, Liu Y and Shuang W 2021 Toward atmospheric electricity research: a low-cost, highly sensitive and robust balloon-borne electric field sounding sensor *IEEE Sens. J.* **21** 13405–16

[11] Giles Harrison R, Nicoll K A, Marlton G J, Tilley D J and Iravani P 2022 Ionic charge emission into fog from a remotely piloted aircraft *Geophys. Res. Lett.* **49** e2022GL099827

[12] Bailey W H, Weil D E and Stewart J R 1997 HVDC power transmission environmental issues review *Technical Report* (Oak Ridge National Lab.(ORNL), Oak)

[13] Biasotto L D and Kindel A 2018 Power lines and impacts on biodiversity: a systematic review *Environ. Impact Assess. Rev.* **71** 110–9

[14] Jonassen N 2013 *Electrostatics* (Springer)

[15] Kluever C A 2015 *Dynamic Systems: Modeling, Simulation and Control* (Wiley)

[16] Priest T, Scelsi G and Woolsey G 1997 Optical fiber sensor for electric field and electric charge using low-coherence, Fabry–Perot interferometry *Appl. Opt.* **36** 4505–8

[17] Kainz A *et al* 2019 Noninvasive 3D field mapping of complex static electric fields *Phys. Rev. Lett.* **122** 6

[18] Han Z, Jun H, Licheng Li and Jinliang H 2023 Micro-cantilever electric field sensor driven by electrostatic force *Engineering* **24** 184–91

[19] Isik S 2023 Analysis of an enclosure for a MEMS DC electric field sensor *Master's Thesis* The University of Manitoba

[20] Liyanage S 2017 A Micromachined DC electric field sensor using a torsional micro mirror *mathesis* The University of Manitoba

[21] Kainz A, Hortschitz W, Kahr M, Keplinger F and Diendorfer G 2020 Microsensor for atmospheric electric fields *EGU General Assembly 2020*

[22] Chen T 2013 Mem electric field sensor using force deflection with capacitance interrogation *2013 IEEE Power And Energy Society General Meeting* pp 1–4

[23] Zhu T, Zhou L, Liu M, Zhang J and Shi L 2015 High sensitive space electric field sensing based on micro fiber interferometer with field force driven gold nanofilm *Sci. Rep.* **5** 15802

[24] Kainz A, Steiner H, Schalko J, Jachimowicz A, Kohl F, Stifter M, Beigelbeck R, Keplinger F and Hortschitz W 2018 Distortion-free measurement of electric field strength with a MEMS sensor *Nat. Electron.* **1** 68–73

[25] Kainz A, Hortschitz W, Steiner H, Stifter M, Schalko J, Jachimowicz A and Keplinger F 2018 Passive optomechanical electric field strength sensor with built-in vibration suppression *Appl. Phys. Lett.* **113** 143505
[26] Kainz A, Steiner H, Hortschitz W, Schalko J, Jachimowicz A and Keplinger F 2019 Improved reference-free vibration-suppressed optical MEMS electric field strength sensor *2019 20th Int. Conf. on Solid-State Sensors, Actuators and Microsystems & Eurosensors XXXIII (Transducers & Eurosensors XXXIII)* (IEEE) pp 2114–7
[27] Li J, Liu J, Peng C, Liu X, Wu Z and Zheng F 2022 Design and testing of a non-contact MEMS voltage sensor based on single-crystal silicon piezoresistive effect *Micromachines* **13** 619
[28] Liao W, Yang Q, Kun K, Qiu Z, Lei Y and Jiao F 2023 Non-intrusive voltage-inversion measurement method for overhead transmission lines based on near-end electric-field integration *Energies* **16** 3415
[29] Huang J'ao, Xiaoming W, Wang X, Yan X and Lin L 2015 A novel high-sensitivity electrostatic biased electric field sensor *J. Micromech. Microeng.* **25** 095008
[30] Xiaoming W *et al* 2017 A sensitivity-enhanced electric field sensor with electrostatic field bias *2017 IEEE Sensors* (IEEE) pp 1–3
[31] Roncin A 2004 *Design of a Microelectromechanical Transducer for Electric Field Measurement. Mathesis* (The University of Manitoba)
[32] Roncin A, Shafai C and Swatek D R 2005 Electric field sensor using electrostatic force deflection of a micro-spring supported membrane *Sens. Actuators* A **123-124** 179–84
[33] Liyanage S, Shafai C, Chen T and Rajapakse A 2017 Torsional moving electric field sensor with modulated sensitivity and without reference ground *Proceedings* **1** 350
[34] Kirkham H, Johnston A, Jackson S and Sheu K 1987 AC and DC Etectric Field Meters Developed for the US *Department of Energy. JPL Publication 87-20, DOE/IET29372-7*
[35] Chubb J 2015 Limitations on the performance of 'field mill' fieldmeters with alternating electric fields *J. Electrost.* **78** 1–3
[36] Bateman M G, Stewart M F, Podgorny S J, Christian H J, Mach D M, Blakeslee R J, Bailey J C and Daskar D 2007 A low-noise, microprocessor-controlled, internally digitizing rotating-vane electric field mill for airborne platforms *J. Atmos. Ocean. Technol.* **24** 1245–55
[37] Jiang H, Zhou B and Yanxin Li 2009 The latest design and development of the field mill used as atmospheric electric field sensor *2009 5th Asia-Pacific Conf. on Environmental Electromagnetics* (IEEE)
[38] Liu C, Yuan H, Jianxun Lv, Zhao P, Jinmeng Li and Hai X 2023 A sensor for 3-D component measurement of synthetic electric field vector in HVDC transmission lines using unidirectional motion *IEEE Trans. Instrum. Meas.* **72** 1–10
[39] Mazur V, Ruhnke L H and Rudolph T 1987 Effect of E-field mill location on accuracy of electric field measurements with instrumented airplane *J. Geophys. Res.* **92** 12013
[40] Clark J F 1957 Airborne measurement of atmospheric potential gradient *J. Geophys. Res.* **62** 617–28
[41] Nicoll K A *et al* 2019 A global atmospheric electricity monitoring network for climate and geophysical research *J. Atmos. Sol.-Terr. Phys.* **184** 18–29
[42] Anisimov S V, Mareev E A, Shikhova N M and Dmitriev E M 2002 Universal spectra of electric field pulsations in the atmosphere *Geophys. Res. Lett.* **29** 70–1–70–4
[43] Harrison G 2002 Twentieth century secular decrease in the atmospheric potential gradient *Geophys. Res. Lett.* **29** 5–1–5–4
[44] Giles Harrison R, Nicoll K A and Aplin K L 2017 Evaluating stratiform cloud base charge remotely *Geophys. Res. Lett.* **44** 6407–12
[45] Jinmeng Li, Zhao P, Yuan H, Jianxun Lv, Liu C and Hai X 2023 Differential structure to improve performance of DC electric field sensors *IEEE Sens. J.* **23** 9909–16
[46] Fort A, Mugnaini M, Vignoli V, Rocchi S, Perini F, Monari J, Schiaffino M and Fiocchi F 2011 Design, modeling and test of a system for atmospheric electric field measurement *IEEE Trans. Instrum. Meas.* **60** 2778–85
[47] Hill D and Kanda M 1999 *The Measurement, Instrumentation and Sensors Handbook XXV* (*Electric Field Strength*) ch 47
[48] Struminsky V I 2000 Vibrational Fluxmeters - A New Class of Electric Field Sensors *Proc. Electrostatics Soc. America, Annual Meeting* pp 108–14
[49] Hill D and Kanda M 1999 *The Measurement, Instrumentation, and Sensors Handbook XXV* (*Instrumentation and Measurements*) (CRC Press LLC) ch 6
[50] Johnston A R, Kirkham H and Bjorn T 1986 Eng. dc electric field meter with fiber-optic readout *Rev. Sci. Instrum.* **57** 2746–53
[51] Bennett A J and Harrison R G 2007 Atmospheric electricity in different weather conditions *Weather* **62** 277–83
[52] Campbell Scientific Inc 2018 Manual - lw110 lightning warning system (available at: https://s.campbellsci.com/documents/us/product-brochures/b_lw110.pdf) (Accessed 21 September 2023)
[53] Chubb J 2010 *An Introduction to Electrostatic Measurements* (Nova Science Publishers)
[54] Zhang B, Wang W and Jinliang H 2015 Impact factors in calibration and application of field mill for measurement of DC electric field with space charges *CSEE J. Power Energy Syst.* **1** 31–36
[55] Antunes de Sá A, Marshall R, Sousa A, Viets A and Deierling W 2020 An array of low-cost, high-speed, autonomous electric field mills for thunderstorm research *Earth Space Sci.* **7** e2020EA001309
[56] Giles Harrison R and Marlton G J 2020 Fair weather electric field meter for atmospheric science platforms *J. Electrost.* **107** 103489
[57] Geonica Manual—Model GEO-EFM-100 electric field mill (available at: www.geonica.com/en/pdf/9755-0032-model-geo-efm-100-electric-field-mill.pdf (Accessed 30 September 2023)
[58] Previstorm 2020 Manual—Previstorm Thunderstorm Warning System (Accessed 30 September 2023)
[59] Chubb J N 1990 Two new designs of field mill type fieldmeters not requiring earthing of rotating chopper *IEEE Trans. Ind. Appl.* **26** 1178–81
[60] Dekra 2019 Manual—JCI Electrostatic Instrumentation—The Measure of Static (Accessed 30 September 2023)
[61] Cui Y, Yuan H, Song X, Zhao L, Liu Y and Lin L 2018 Model, design and testing of field mill sensors for measuring electric fields under high-voltage direct-current power lines *IEEE Trans. Ind. Electron.* **65** 608–15
[62] Shahroom H, Buntat Z, Sidik M A B, Nawawi Z and Jambak M I 2015 Atmospheric electric field measurement advances in southern peninsular Malaysia *2015 IEEE Conf. on Energy Conversion (CENCON)* pp 116–21
[63] Fort A, Mugnaini M, Vignoli V, Rocchi S, Perini F, Monari J, Schiaffino M and Fiocchi F 2010 Design and modeling of an optimized sensor for atmospheric electric field measurement *2010 IEEE Sensors Applications Symp. (SAS)* (IEEE)

[64] Mission Instruments Co. 2020 Manual—EFS 1000 series electric field mill (Accessed 30 September 2023)
[65] Horenstein M N and Stone P R 2001 A micro-aperture electrostatic field mill based on MEMS technology *J. Electrost.* **51–52** 515–21
[66] Riehl P S, Scott K L, Muller R S, Howe R T and Yasaitis J A 2003 Electrostatic charge and field sensors based on micromechanical resonators *J. Microelectromech. Syst.* **12** 577–89
[67] Lundberg K H, Shafran J S, Kuang J, Judy M and Denison T A 2006 A self-resonant MEMS-based electrostatic field sensor *2006 American Control Conf.* p 6
[68] Denison T, Kuang J, Shafran J, Judy M and Lundberg K 2006 A self-resonant MEMS-based electrostatic field sensor with 4V/m/Hz sensitivity *2006 IEEE Int. Solid State Circuits Conf. - Digest of Technical Papers* pp 1121–30
[69] Sawa Shafran J 2005 A MEMS-based, high-resolutionelectric-field meter *Master's Thesis* Massachusetts Institute of Technology
[70] Chen X, Peng C, Tao H, Chao Y, Bai Q, Chen S and Xia S 2006 Thermally driven micro-electrostatic fieldmeter *Sens. Actuators* A **132** 677–82
[71] Denison T A, Shafran J S, Kuang J and Lundberg K H 2007 A self-resonant MEMS-based electrometer *2007 IEEE Instrumentation and Measurement Technology Conf. IMTC 2007* pp 1–5
[72] Peng S, Zhang Z, Liu X, Gao Y, Zhang W, Xing X, Liu Y, Peng C and Xia S 2023 A single-chip 3-D electric field microsensor with piezoelectric excitation *IEEE Trans. Electron Devices* **70** 4359–65
[73] Chu Z, Yang P, Wen X and Peng C 2023 A resonant electrostatic field microsensor with self-compensation for sensitivity drift *IEEE Sens. J.* **23** 13917–24
[74] Ghionea S, Smith G, Pulskamp J, Bedair S, Meyer C and Hull D 2013 MEMS electric-field sensor with lead zirconate titanate (PZT)-actuated electrodes *SENSORS, 2013 IEEE* (IEEE) pp 1–4
[75] Wang Z, Zhengwei W, Liu X, Gao Y, Peng S, Ren R, Zheng F, Yao Lv and Peng C 2021 A novel high sensitive mode-localization MEMS electric field sensor based on closed-loop feedback *2021 21st Int. Conf. on Solid-State Sensors, Actuators and Microsystems (Transducers)* pp 423–6
[76] Peng C, Yang P, Zhang H, Guo X and Xia S 2010 Design of a SOI MEMS resonant electric field sensor for power engineering applications *SENSORS, 2010 IEEE* pp 1183–6
[77] Liu X *et al* 2021 Enhanced sensitivity and stability of a novel resonant MEMS electric field sensor based on closed-loop feedback *IEEE Sens. J.* **21** 22536–43
[78] Ling B, Wang Y, Peng C, Li B, Chu Z, Li B and Xia S 2017 Design, fabrication and characterization of a single-chip three-dimensional electric field microsensor *2017 IEEE 12th Int. Conf. on Nano/Micro Engineered and Molecular Systems (NEMS)* (IEEE) pp 307–10
[79] Baxter L K 1997 Capacitive sensors *Design and Applications* (IEEE press) pp 9–14
[80] 2023 Ppm test, prodyn free space electric field (d-dot) sensors (available at: https://ppmtest.com/products/e-field-sensors/prodyn-electric-field-sensors/free-space-electric-field-sensors) (Accessed 30 September 2023)
[81] Montena 2023 Field sensors (available at: www.montena.com/system/pulse-measurement-fibre-optic-links/field-sensors)
[82] 2020 IEEE standard procedures for measurement of power frequency electric and magnetic fields from AC power lines *IEEE Std 644-2019 (Revision of IEEE Std 644-2008)* pp 1–40
[83] General Systems Subcommittee 1978 Measurement of electric and magnetic fields from alternating current power lines *IEEE Trans. Power Appar. Syst.* **PAS-97** 1104–14
[84] Manual—Narda, 'EFA-200/-300 EM Field Analyzer. Operating Manual (Accessed 25 September 2023)
[85] Manual—Maschek, 3D H/E fieldmeter ESM 100 Produktdatenblatt (Accessed 25 September 2023)
[86] Manual—Wavecontrol, WP400 Probe Datasheet (Accessed 25 September 2023)
[87] Manual—TREK Iinc, Trek Model 347 Electrostatic Voltmeter (Accessed 21 September 2023)
[88] Manual—Panasonic Industrial Devices, Electrostatic Sensor EF-S1 SERIES (Accessed 21 September 2023)
[89] Manual—Keyence Corporation of America, Electrostatic Sensor—SK series (Accessed 21 September 2023)
[90] Kobayashi T, Oyama S, Takahashi M, Maeda R and Itoh T 2008 Microelectromechanical systems-based electrostatic field sensor using Pb(Zr,Ti)O_3 thin films *Japan. J. Appl. Phys.* **47** 7533
[91] Kobayashi T, Oyama S, Okada H, Makimoto N, Tanaka K, Itoh T and Maeda R 2012 An electrostatic field sensor driven by self-excited vibration of sensor/actuator integrated piezoelectric micro cantilever *2012 IEEE 25th Int. Conf. on Micro Electro Mechanical Systems (MEMS)* (IEEE) pp 527–30
[92] Kobayashi T, Oyama S, Makimoto N, Okada H, Itoh T and Maeda R 2013 An electrostatic field sensor operated by self-excited vibration of MEMS-based self-sensitive piezoelectric microcantilevers *Sens. Actuators* A **198** 87–90
[93] Bordovsky 1998 Electrooptic electric field sensor for dc and extra-low-frequency measurement *PhD Thesis* Department of Manufacturing and Engineering Systems, Brunel University
[94] Duvillaret L, Rialland S and Coutaz J-L 2002 Electro-optic sensors for electric field measurements. i. theoretical comparison among different modulation techniques *J. Opt. Soc. Am.* B **19** 2692–703
[95] Toney J E, Stenger V E, Kingsley S A, Pollick A, Sriram S and Taylor E 2012 Advanced materials and device technology for photonic electric field sensors *Proc. SPIE* **8519** 11–22
[96] Rogers A J 1979 Optical measurement of current and voltage on power systems *IEE J. Electr. Power Appl.* **2** 120–4
[97] Gaborit G, Artillan P, Bermond C, Revillod G, Chevrier-Gros G and Duvillaret L 2020 20 GHz antenna radiation pattern obtained from near-field mapping with electrooptic probe on a single plane *IEEE Antennas Wirel. Propag. Lett.* **19** 1177–81
[98] Mazzola M S, Schoenbach K H and Peterkin F E 1995 Gallium-arsenide optically isolated electric field sensor for utility and pulsed power applications *Digest of Technical Papers. 10th IEEE Int. Pulsed Power Conf.* vol 1 pp 372–7
[99] Cheng W-C, Chiu Y-J and Kao F-J 2005 Electric field probing by incorporating Franz-Keldysh electroabsorption effect and optical-beam-induced-current technique *2005 IEEE LEOS Annual Meeting Conf. Proc.* pp 901–2
[100] Brinkmann M *et al* 2007 *Optical Materials and Their Properties* (Springer) pp 249–372
[101] Maeno T and Takada T 1987 Electric field measurement in liquid dielectrics using a combination of AC voltage modulation and a small retardation angle *IEEE Trans. Electr. Insul.* **EI–22** 503–8
[102] Rose A H, Etzel S M and Rochford K B 1999 Optical fiber current sensors in high electric field environments *J. Lightwave Technol.* **17** 1042–8
[103] Okubo H 2018 HVDC electrical insulation performance in oil/pressboard composite insulation system based on kerr

electro-optic field measurement and electric field analysis *IEEE Trans. Dielectr. Electr. Insul.* **25** 1785–97

[104] Onishi D, Kumada A, Hidaka K, Umemoto T, Otake Y and Tsurimoto T 2017 Surface potential measurement of stress grading system of high voltage rotating machine coils using pockels field sensor *2017 Int. Symp. on Electrical Insulating Materials (ISEIM)* vol 1 pp 95–98

[105] Hidaka K 1996 Progress in Japan of space charge field measurement in gaseous dielectrics using a pockels sensor *IEEE Electr. Insul. Mag.* **12** 17–28

[106] Gaborit G, Fond E, Bouhriz H, Chevrier-Gros G and Duvillaret L 2023 Partial discharge assessment using optical probe *2023 IEEE Electrical Insulation Conf. (EIC)* pp 1–4

[107] Peng J, Jia S, Bian J, Zhang S, Liu J and Zhou X 2019 Recent progress on electromagnetic field measurement based on optical sensors *Sensors* **19** 2860

[108] Grasdijk J O, Bai X F A U, Engin I, Jungmann K, Krause H J, Niederländer B, Offenhäuser A, Repetto M, Willmann L and Zimmer S 2019 Electro-optic sensor for static fields *Appl. Phys.* B **125** 212

[109] Kumada A and Hidaka K 2013 Directly high-voltage measuring system based on pockels effect *IEEE Trans. Power Deliv.* **28** 1306–13

[110] He B, Liu S, Zhu P, Yifei Li and Cui D 2018 The working characteristics of electric field measurement based on the pockels effect for AC–DC hybrid fields *Meas. Sci. Technol.* **29** 125004

[111] Cecelja F, Bordovsky M and Balachandran W 2001 Lithium niobate sensor for measurement of DC electric fields *IEEE Trans. Instrum. Meas.* **50** 465–9

[112] Cecelja F, Bordovsky M and Balachandran W 2002 Electro-optic sensor for measurement of DC fields in the presence of space charge *IEEE Trans. Instrum. Meas.* **51** 282–6

[113] Cecelja F, Balachandran W and Bordowski M 2007 Validation of electro-optic sensors for measurement of DC fields in the presence of space charge *Measurement* **40** 450–8

[114] Jarzynski J and De Paula R P 1987 Fiber Optic Electric Field Sensor Technology *Proc. SPIE* **0718** 48–55

[115] Chmielak B, Waldow M, Matheisen C, Ripperda C, Bolten J, Wahlbrink T, Nagel M, Merget F and Kurz H 2011 Pockels effect based fully integrated, strained silicon electro-optic modulator *Opt. Express* **19** 17212–9

[116] Zeng R, Wang B, Niu B and Zhanqing Y 2012 Development and application of integrated optical sensors for intense E-field measurement *Sensors* **12** 11406–34

[117] Toney J E, Tarditi A G, Pontius P, Pollick A, Sriram S and Kingsley S A 2014 Detection of energized structures with an electro-optic electric field sensor *IEEE Sens. J.* **14** 1364–9

[118] Zhang J, Chen F, Sun B and Chen K 2014 Integrated optical waveguide sensor for lighting impulse electric field measurement *Photonic Sens.* **4** 215–9

[119] Zhang J, Chen F, Sun B, Chen K and Li C 2014 3D integrated optical E-field sensor for lightning electromagnetic impulse measurement *IEEE Photonics Technol. Lett.* **26** 2353–6

[120] Zhang X, Hosseini A, Subbaraman H, Wang S, Zhan Q, Luo J, Jen A K and Chen R T 2014 Integrated photonic electromagnetic field sensor based on broadband bowtie antenna coupled silicon organic hybrid modulator *J. Lightwave Technol.* **32** 3774–84

[121] Wackernagel D, Kaufmann F, Maeder A, Grange R and Franck C M 2023 Integration of an optical electric field sensor in lithium niobate on insulator *IEEE Access* **11** 90715–23

[122] SRICO Manual—Photonic Electric Field Sensor System Model 200-04 (Accessed 21 September 2023)

[123] Ma X Q, He K, Lu J Y, Xie L, Ju Y, Zhao L X and Gao W S 2021 Effects of temperature and humidity on ground total electric field under HVDC lines *Electr. Power Syst. Res.* **190** 106840

[124] Muller P O, Alleston S B, Vickers A J and Erasme D 1999 An external electrooptic sampling technique based on the Fabry-Perot effect *IEEE J. Quantum Electron.* **35** 7–11

[125] Gillette L, Gaborit G, Volat C, Dahdah J, Lecoche F, Jarrige P and Duvillaret L 2014 Optical sensor for the diagnostic of high voltage equipment *2014 IEEE Electrical Insulation Conf. (EIC)* pp 142–6

[126] Bernier M, Duvillaret L, Gaborit G, Paupert A and Lasserre J 2009 Fully automated E-field measurement system using pigtailed electro-optic sensors for temperature-dependent-free measurements of microwave signals in outdoors conditions *IEEE Sens. J.* **9** 61–68

[127] Owens I, Grabowski C, Biller A, Ulmen B, Joseph N, Hughes B, Coffey S, Kirschner D and Struve K 2021 Electro-optical measurement of intense electric field on a high energy pulsed power accelerator *Sci. Rep.* **11** 10702

[128] Zhang J and Lei H 2023 Design of a lithium niobate electric field sensor with improved sensitivity *Sens. Actuators* A **362** 114611

[129] Hoffman C and Driggers R 2015 *Encyclopedia of Optical and Photonic Engineering (Print)-Five Volume Set* (CRC Press)

[130] Kaminow I P 2013 *An Introduction to Electrooptic Devices: Selected Reprints and Introductory Text By* (Academic)

[131] Sato M, Kumada A, Hidaka K, Yamashiro K, Hayase Y and Takano T 2014 On the nature of surface discharges in silicone-gel: Prebreakdown discharges in cavities *2014 IEEE Conf. on Electrical Insulation and Dielectric Phenomena (CEIDP)* pp 19–22

[132] Kuo W-K, Chen W-H, Huang Y-T and Huang S-L 2000 Two-dimensional electric-field vector measurement by a $LiTaO_3$ electro-optic probe tip *Appl. Opt.* **39** 4985–93

[133] Volat C, Duvillaret L, Lecoche F, Dahdah J and Gaborit G 2013 Contactless optical sensors for in situ AC and DC electric field measurement and diagnostics *2013 IEEE Electrical Insulation Conf. (EIC)* pp 365–9

[134] Gaborit G, Dahdah J, Lecoche F, Jarrige P, Gaeremynck Y, Duraz E and Duvillaret L 2013 A nonperturbative electrooptic sensor for in situ electric discharge characterization *IEEE Trans. Plasma Sci.* **41** 2851–7

[135] Perry D, Chadderdon S, Richard Gibson B S, Selfridge R H, Schultz S M, Wang W C, Forber R and Luo J 2011 Electro-optic polymer electric field sensor *Proc. SPIE* **7982** 230–7

[136] Zhou J, Liu J, Wang M, Hou W, Qin G, Kityk I V, Fedorchuk A A, Albassam A A, El-Naggar A M and ndrushchak A A 2017 Novel poly (aryl ether ketone) with electro-optic chromophore side chains for light modulators *J. Mater. Sci., Mater. Electron.* **28** 18568–77

[137] Zeng Z, Liu J, Luo T, Zhibei Li, Liao J, Zhang W, Zhang L and Liu F 2022 Electro-optic crosslinkable chromophores with ultrahigh electro-optic coefficients and long-term stability *Chem. Sci.* **13** 13393–402

[138] Xu H, Liu J, Liu J, Canwen Y, Zhai Z, Qin G and Liu F 2020 Self-assembled binary multichromophore dendrimers with enhanced electro-optic coefficients and alignment stability *Mater. Chem. Front.* **4** 168–75

[139] Luo M, Yang Q, Dong F, Chen N and Liao W 2021 Miniature micro-ring resonator sensor with electro-optic polymer cladding for wide-band electric field measurement *J. Lightwave Technol.* **40** 2577–84

[140] Kondo R, Yoshimura K, Hachisu Y, Hyeon-Gu J, Fujii M, Ihori H, Otake Y, Umemoto T and Tsurimoto T 2017

Measurement of AC electric field in transformer oil using kerr effect *2017 Int. Symp. on Electrical Insulating Materials (ISEIM)* vol 1 pp 255–8
[141] Zhang X, Kendall Nowocin J and Zahn M 2013 Experimental determination of the valid time range for kerr electro-optic measurements in transformer oil stressed by high-voltage pulses *2013 Annual Report Conf. on Electrical Insulation and Dielectric Phenomena* pp 522–6
[142] Nassar M, Daaboul M, Michel A and Louste C 2023 Electro-optical kerr effect in HFE-7100 *2023 IEEE 22nd Int. Conf. on Dielectric Liquids (ICDL)* pp 1–4
[143] Okubo H, Nara T, Saito H, Kojima H, Hayakawa N and Kato K 2010 Breakdown characteristics in oil/pressboard composite insulation system at HVDC polarity reversal *2010 Annual Report Conf. on Electrical Insulation and Dielectric Phenomena* pp 1–4
[144] Duvillaret L, Rialland S and Coutaz J-L 2002 Electro-optic sensors for electric field measurements. II. Choice of the crystals and complete optimizatino of their orientation *J. Opt. Soc. Am.* B **19** 2704–15
[145] Gaborit G, Jarrige P, Dahdah J, Gillette L and Duvillaret L 2015 Packaged optical sensors for the electric field characterization in harsh environments *2015 Int. Conf. on Electromagnetics in Advanced Applications (ICEAA)* pp 1468–71
[146] Zhang Y, Zhang J, Li Y and Lei H 2022 An optical intense 2D electric field sensor using a single $LiNO_3$ crystal *Curr. Opt. Photon.* **6** 183–90
[147] Manual - Seikoh-Giken - Isotropic Optical E-field Sensor Head (Accessed 25 September 2023)
[148] Garzarella A, Qadri S B and Ho Wu D 2009 Optimal electro-optic sensor configuration for phase noise limited, remote field sensing applications *Appl. Phys. Lett.* **94** 221113
[149] Robertson S R M and Rogers A J 1985 Measurement of DC electric fields using the electro-optic effect *IEE Proc. J. Optoelectron.* vol 132 pp 195–8
[150] Garzarella A, Qadri S B, Ho Wu D and Hinton R J 2007 Responsivity optimization and stabilization in electro-optic field sensors *Appl. Opt.* **46** 6636–40
[151] Yang Q, Liu R, Yanxiao H and Luo M 2020 AC/DC hybrid electric field measurement method based on Pockels effect and electric field modulation *Rev. Sci. Instrum.* **91** 055004
[152] 1990 Ieee guide for the measurement of DC electric-field strength and ion related quantities *IEEE Std 1227-1990* pp 1–54
[153] Lasta Fritzen C, Alves Fernandes W, Carlos Notari A, Moreschi Dias W, Macedo Rescigno G, Rangel Rodrigues T and Lacerda M 2019 Electric field sensor calibration using horizontal parallel plates *2019 Int. Symp. on Lightning Protection (XV SIPDA)* (IEEE)
[154] Elizabeth Catherine A, James N, Ruben Waldo S, and Alan H 2017 Uncertainty analysis of an electric field mill calibration system *Technical Report* (Sandia National Lab.(SNL-NM))
[155] Mou Y, Zhanqing Y, Fan Y, Zhang B, Zhang C, Wang X, Zeng R and Jinliang H 2019 Calibration of a sensor for an ion electric field under HVDC transmission lines *J. Eng.* **2019** 2842–5
[156] Zhang B, Wang W, Jinliang H, Zeng R and Yin H 2012 Calibration of field-mill instrument for measuring DC electric field *2012 Int. Conf. on High Voltage Engineering and Application* (IEEE)
[157] Zhang B, Wei Li, Zeng R and Jinliang H 2013 Study on the field effects under reduced-scale DC/AC hybrid transmission lines *IET Gener. Transm. Distrib.* **7** 717–23
[158] Sellars M 1995 Electric field mill for the simultaneous measurement of electric field strength and ion current diensity *Mathesis* University of Cape Town
[159] Yansong Li, Gao Li, Wan J and Liu J 2020 Optical DC electric field sensing based on the Pockels effect using bismuth germanate crystals *Appl. Opt.* **59** 6237–44
[160] Hidaka K and Fujita H 1982 A new method of electric field measurements in corona discharge using pockels device *J. Appl. Phys.* **53** 5999–6003
[161] Liu J, Wang H and Yansong Li 2019 Research and design of rotary optical electric field sensor *IOP Conf. Ser.: Mater. Sci. Eng.* **677** 052112
[162] Wang H, Zeng R, Zhuang C, Lyu G, Junjie Y, Niu B and Chanxiao Li 2020 Measuring AC/DC hybrid electric field using an integrated optical electric field sensor *Electr. Power Syst. Res.* **179** 106087
[163] Dallaire R D and Sarma Maruvada P 1987 Corona performance of a $\pm$ 450-kV bipolar DC transmission line configuration *IEEE Trans. Power Deliv.* **2** 477–85
[164] Xinyu M, Zhuang C, Zeng R and Zhou W 2020 Large-dynamic-range athermal lithium niobite on insulator/TiO_2 nanobeam electric field sensor *J. Phys. D: Appl. Phys.* **54** 105101
[165] Cui Y, Song X, Wang C, Zhao L and Wu G 2020 Ground-level DC electric field sensor for overhead HVDC/HVAC transmission lines in hybrid corridors *IET Gener. Transm. Distrib.* **14** 4173–4178